

Acknowledgement. The financial support from the Ministry of Education through the Research Institute for Basic Science is greatly appreciated.

References

1. J. J. Lingane, *Ind. Eng. Chem. Ed.*, **15**, 584 (1943).
2. K. H. Koh, *J. Kora. Chem. Soc.*, **11**, 179 (1967).
3. B. Csiszar and P. Szarvas, *Nature* **3**, 846 (1960).
4. D. D. DeFord and D. L. Andersen, *J. Am. Chem. Soc.* **72**, 3918 (1950).
5. D. N. Hume, D. D. DeFord, and G. C. B. Cave, *J. Am. Chem. Soc.*, **73**, 5323 (1951).
6. O. I. Komolev and Z. G. Galanets, *Chem. Abstra.* **51**, 11906g (1957).
7. R. W. Murray and D. J. Gross, *Anal. Chem.* **38**, 392 (1966).
8. K. K. Tripathy, R. K. Patnaik and S. Pari, *J. Indian Chem. Soc.* **49**, 345 (1972).
9. G. L. Robbins and R. E. Tapscott, *Inorg. Chem.* **15**, 154 (1976).
10. R. E. Tapscott, R. E. Belford, and I. C. Paul, *Coord. Chem. Rev.*, **4**, 323 (1969).

Electrical Properties of Pure and Cadmium-Doped Indium Sesquioxide

Sung Han Lee, Jong Hwan Lee, and Keu Hong Kim*

Department of Chemistry, Yonsei University, Seoul 120-749

Jong Ho Jun

Department of Biochemistry, Konkuk University, Chungju 380-150. Received March 22, 1989

Cadmium-doped indium sesquioxide systems with a variety of CdO mol % were prepared to investigate the effect of doping on the electrical properties of indium sesquioxide. The electrical conductivities of pure In_2O_3 and Cd-doped In_2O_3 systems were measured in the temperature range from 25 to 1200 °C and P_{O_2} range from 10^{-7} to 10^{-1} atm, and the thermoelectric power was measured in the same temperature range. The electrical conductivity and thermopower decreased with increasing CdO mol % indicating that all the samples are n-type semiconductors. The electrical conductivities of pure In_2O_3 and lightly doped In_2O_3 were considerably affected by the chemisorption O_2 at temperatures of 400 to 560 °C and then gaseous oxygen was reversibly chemisorbed at the temperature. The predominant defects in In_2O_3 are believed to be triply-charged interstitial indiums at temperatures above 560 °C and oxygen vacancies below 560 °C. In Cd-doped In_2O_3 systems, cadmium acts as an electron acceptor and inhibits the transfer of lattice indium to interstitial sites, which give rise to the decrease of the electrical conductivity.

Introduction

Indium sesquioxide has been known to be an n-type semiconductor. Pure and impurity-doped indium sesquioxides find use in a variety of applications such as electrodes in solar cells¹, gas detectors², and heterogeneous oxidation-reduction catalysts^{3,4}. The electrical properties of In_2O_3 along with its defect structure have been extensively studied, but the detailed conduction mechanism is not yet fully understood. Ovadyahu *et al.*⁵ suggested the existence of In atoms with different valences in In_2O_3 based on the results of stoichiometry measurements, Hall effect and crystal structure data. In view of these reports, the electrical conduction mechanism in indium sesquioxide may be more complicated than hitherto assumed.

Indium sesquioxide doped with acceptor or donor impurities is expected to become p-type or a highly resistive n-type due to the compensation effect in wide band gap semiconductors. Wit *et al.*^{6,7} reported that the electrical behavior of In_2O_3 between 25 and 800 °C is influenced by impurities, the impurity effect is overshadowed by intrinsic properties

above 800 °C. Kanai investigated the electrical conduction in a Mg-doped In_2O_3 single crystal between -173 and 25 °C and found that the electrical conduction was electronic with the electron concentration and electron mobility in the crystal almost independent of temperature⁸. Until now, few results have been reported for the electrical properties of indium sesquioxide polycrystals doped with other elements. In the present work, we report on the electrical properties of Cd-doped In_2O_3 systems and suggest the nature of the electrical conduction mechanism based on the results.

Experimental

Sample Preparation. Specpure indium sesquioxide (99.999% pure, Aldrich Co.) and cadmium oxide (99.999% pure, Johnson-Matthey Co.) powders were used for the preparation of Cd-doped In_2O_3 systems. Finely screened CdO and In_2O_3 powders were uniformly dispersed in various mole ratios in pure ethanol for 48 hrs and the mixtures were filtered and dried at 150 °C. CdO- In_2O_3 solid solutions were prepared by allowing direct solid-state reaction between the

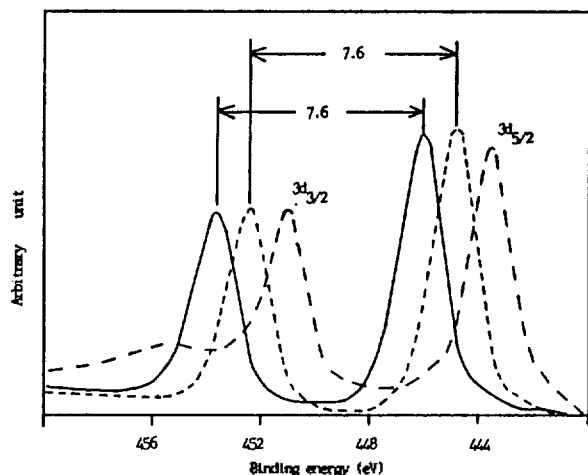


Figure 1. ESCA spectra of In(---), In_2O_3 (99.999%) (----), and In_2O_3 sintered at 1000°C and 1.3×10^{-4} atm (—).

relatively volatile CdO and In_2O_3 at 800°C for 10 hrs and then at 1100°C for 30 hrs in a covered platinum crucible, followed by slow cooling to room temperature at a rate of 50°C/hr in order to minimize oxygen defects. The powder so obtained was dispersed in 10% aqueous ammonia in order to remove any uncombined CdO and then dried at 150°C . For identification of phase and structure, X-ray diffractometry was performed on the samples. The lattice parameter, determined for the In_2O_3 bcc solid solutions containing up to 4.8 mol % after heat treatment in air at 1100°C by the Nelson-Riley method, increased from 10.09 \AA for pure In_2O_3 to 10.12 \AA at 4.8 mol % CdO , indicating the present specimens are solid solutions. The amount of CdO dopant was determined by inductively coupled plasma emission spectrographic analysis. To investigate the structure of surface phases on the samples, ESCA spectra were obtained for standard specimens and specimens prepared in this work. The DTA showed that no heat change occurs in the present specimens in the temperature range of 25 to 1200°C .

Measurements. To measure the electrical conductivity, the powders were compressed to pellets under 8 tons/cm^2 in vacuum. The pellet, surrounded by $\text{CdO-In}_2\text{O}_3$ powder of the same composition, was sintered in air at 1100°C for 48 hrs and cooled slowly to room temperature. The sintered density of the pellet was about 90–95% of the theoretical density. The pellets were polished flat using In_2O_3 powder as an abrasive. Before the sample was inserted into the sample container, it was etched in $(\text{NH}_4)_2\text{S}_2\text{O}_8$ and dilute HNO_3 solution, washed with distilled water, dried, and then connected to the Pt probes. The dc conductivity was measured by means of the four-probe method described in the literature⁹. The various oxygen partial pressures required were established using pure oxygen or a mixture of oxygen in nitrogen. The quartz sample container was evacuated to a pressure 1×10^{-4} torr at room temperature, pure oxygen or a mixture of oxygen-nitrogen was then introduced into the sample container, and the total pressure again reduced to achieve the required oxygen pressure. The pressure of the oxygen-nitrogen mixture and the pressure in the evacuated sample container were read on a Penning gauge and an ultra-high-vacuum ionization gauge, respectively. The conductivity was measured with increasing temperature at intervals

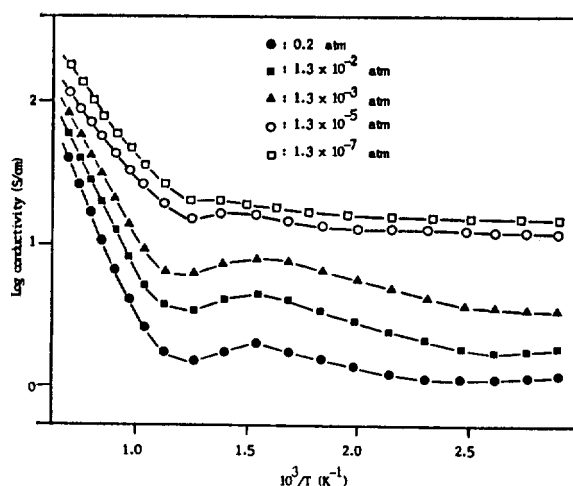


Figure 2. Log conductivity vs. $10^3/T$ for pure In_2O_3 at various P_{O_2} .

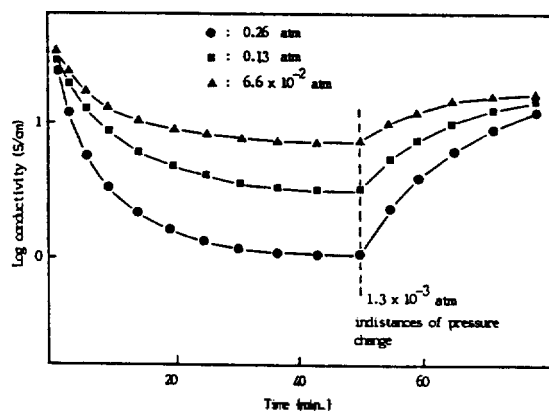


Figure 3. The variation of electrical conductivity of vacuum-treated In_2O_3 with time under various oxygen pressures at 450°C .

of 25°C and each measurement was made after the conductivity reached equilibrium.

To measure the thermoelectric power, the bar-shaped sample was suspended from two Pt/Pt-10% Rh thermocouples whose junctions were attached to the ends of the sample using nickel paste so that good thermal and electrical contact was maintained. A cold finger immediately below the sample was used to impose temperature gradients on the specimen. The thermal emf's generated by the thermal gradients across the sample were measured using a differential voltmeter between the Pt leads of the thermocouples with temperature differences of 10 to 15°C used during each measurement.

Results

Figure 1 shows ESCA spectra of several specimens, in which indium metal peaks are not found in pure In_2O_3 specimens. Peaks for sintered In_2O_3 in vacuum shift by 1.3 eV to an upper position on binding energy. Figure 2 shows log conductivity vs. $1/T$ for pure In_2O_3 at various oxygen partial pressures from 10^{-7} to 10^{-1} atm and temperatures from 25 to 1200°C , in which conductivity peaks appear near 400°C and diminish with decreasing P_{O_2} . Figure 3 shows the conductivity of pure In_2O_3 under various oxygen pressures as a function of time at 450°C . The conductivity gradually decreases with the passage of time and with increasing oxy-

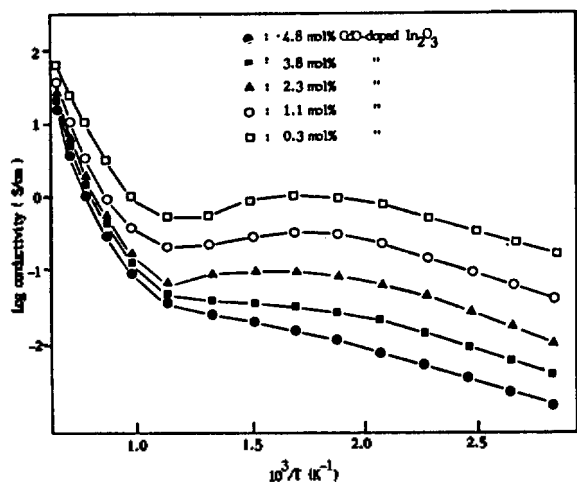


Figure 4. Log conductivity vs. $10^3/T$ for Cd-doped In_2O_3 systems at $P_{\text{O}_2} = 0.2$ atm.

Table 1. Activation Energies for Electrical Conductivity in the pure In_2O_3 and Cd-doped In_2O_3 system

Composition	Activation energy (eV)	
	560–1200 °C	25–560 °C
Pure In_2O_3	1.36	—
0.3 mol% CdO- In_2O_3	1.36	—
1.1 mol% CdO- In_2O_3	1.39	—
2.3 mol% CdO- In_2O_3	1.39	—
3.8 mol% CdO- In_2O_3	1.49	—
4.8 mol% CdO- In_2O_3	1.59	0.24

gen pressure; it then increases again after the container is evacuated.

Figure 4 shows log conductivity values plotted as a function of the reciprocal of absolute temperature for 0.3, 1.1, 2.3, 3.8, and 4.8 mol % Cd-doped In_2O_3 systems in the temperature range from 25 to 1200 °C at P_{O_2} of 2×10^{-1} atm. The curves for the Cd-doped In_2O_3 systems are divided into high- and low-temperature regions. The 4.8 mol % Cd-doped In_2O_3 system shows distinct extrinsic region and the electrical conductivity decreases as the amount of CdO increases. Activation energies obtained by the least-squares method from the conductivity-temperature data for all the samples are given in Table 1. The activation energy, 1.36 eV, obtained for the high temperature region between 560 and 1200 °C for undoped In_2O_3 is in agreement with those of Bockris *et al.*¹⁰ (1.3 eV), Weiher *et al.*¹¹ (1.4 eV), Wit⁷ (1.5 eV), and Vijh¹² (1.6 eV), but shows a difference from those of Dignam *et al.*¹ (1.8 eV) and Granqvist *et al.*¹³ (1.87 eV).

The thermoelectric power for all the specimens is negative and the Seebeck coefficient varies with CdO content as shown in Figure 5. Figure 6 shows that the thermoelectric powder for the 4.8 mol % Cd-doped In_2O_3 was negative in the temperature range from 25 to 1200 °C. Figure 7 shows isobaric conductivity plotted against $1/T$ for the 4.8 mol % Cd-doped In_2O_3 system; the temperature dependence of the electrical conductivity shows typical intrinsic and extrinsic properties.

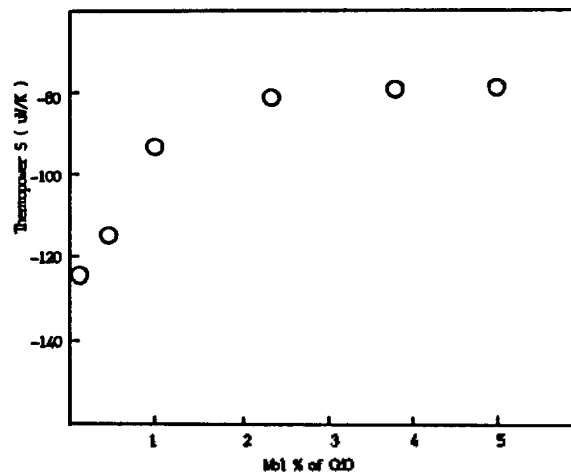


Figure 5. Thermopower S vs. CdO concentration at 1073 K in air pressure.

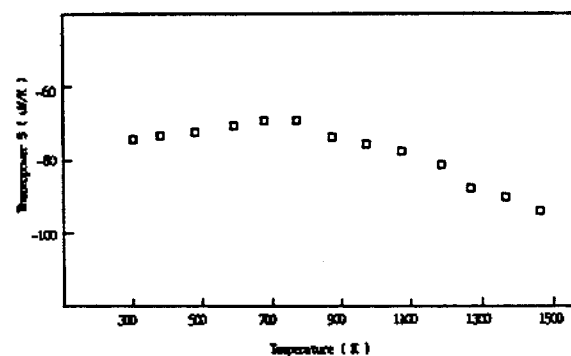


Figure 6. Thermopower S vs. temperature for 4.8 mol% Cd-doped In_2O_3 in air pressure.

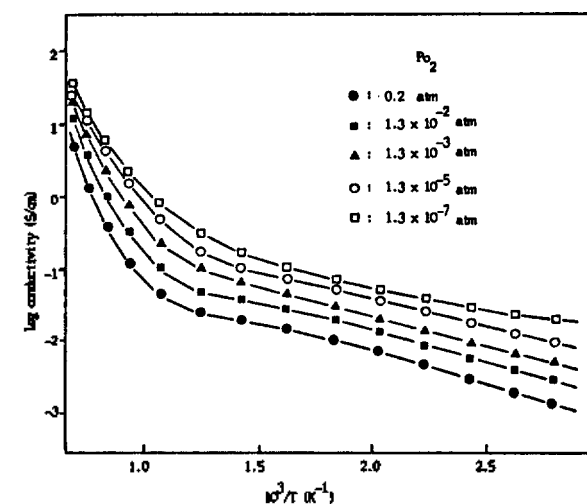


Figure 7. Log conductivity vs. $10^3/T$ of 4.8 mol% Cd-doped In_2O_3 at various P_{O_2} .

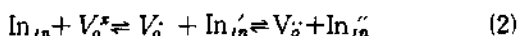
Discussion

As shown in Figure 2, electrical conductivity maximum appeared around 400 °C and the peak diminished at lower oxygen partial pressures. The conductivity under oxygen gas gradually decreased with time, but increased again when the

sample container was evacuated as shown in Figure 3. These results indicate that the presence of gaseous oxygen is the main cause of the changes in the electrical conductivity. Wit *et al.*¹⁴ measured the mobility in the polycrystalline In_2O_3 as a function of increasing temperature in the range from 25 to 700°C and found that the mobility was nearly constant in the temperature range. From these results, it is believed that the change in conductivity is governed mainly by the change in carrier concentration so that the temperature dependence of the mobility can be neglected comparing to the temperature dependence of the carrier concentration in the range of 25 to 700°C. From Figure 3, it is clear that oxygen molecules can be reversibly chemisorbed on the surface of In_2O_3 at 450°C. When gaseous oxygen is chemisorbed, the electron concentration should be decreased because the chemisorbed O_2 dissipates conduction electrons in the semiconductor. In a previous paper⁴, we reported that under P_{CO} the conductivities of In_2O_3 and 8 mol % Ni-doped In_2O_3 increased with increasing CO pressure. In_2O_3 loses some oxygen from lattice sites under reducing conditions and the indium oxide then can be described by



In Figure 1, the shift of peaks for In_2O_3 sintered at 1000°C in vacuum to an upper position is due to deficiency of oxygen. Many investigators have reported that oxygen vacancies can be produced by heating In_2O_3 ¹⁴⁻¹⁶ and these agree with the present result. The oxygen vacancy can act as a donor and can become singly or doubly charged. The free electrons may also be associated with or localized at normal cation sites and the equation may then be written as

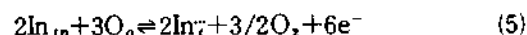


In fact, the existence of lower valence indium ions in indium oxide was reported, especially the existence of In^{1+} under mild conditions^{5,17}. Also, the oxygen vacancy ($\text{V}_\text{o}^{\bullet\bullet} - 2e^-$) can act as an adsorption site for oxygen molecule⁴. When O_2 is adsorbed on the surface, the electrical conductivity should decrease with increasing P_{O_2} as shown in Figure 3. Therefore, it is believed from Figures 2 and 3 that oxygen vacancies are predominant at temperatures below 560°C and the electron concentration in In_2O_3 then are considerably affected by oxygen-surface interaction.

On the other hand, in the high temperature region above 560°C, the electrical conductivity curve for pure In_2O_3 is typical of that for intrinsic conductivity. The donor levels in In_2O_3 are located around 0.01 eV just below the conduction band¹⁸ and thus electrons can be easily excited to the conduction band. Thus, it is believed that the activation energy, 1.36 eV, obtained in the temperature range from 560 to 1200°C consists of the energy for carrier migration, the energy for the transfer of In_{In} atoms to an interstitial site, and the energy for the formation of oxygen vacancies. In an oxygen deficient oxide, the predominant defects may constitute interstitial metal atoms. In In_2O_3 , the neutral In_i^0 atoms may be successively ionized to singly charged, doubly charged or triply charged interstitial ions as in Eq. (3), resulted in the increase of concentration of conduction electron.



Interstitial indiums in indium oxide have been suggested in some recent report.^{5,17} Considering the formation of oxygen vacancy and interstitial indium as defects, the defect equations may be written as



Based on the electroneutrality condition, when $[\text{V}_\text{o}^{\bullet\bullet}] \gg [\text{In}_i^+]$ then

$$[e^-] = (2K_4)^{1/3} P_{\text{O}_2}^{-1/6} \quad (6)$$

$$[\text{In}_i^+] = (K_5)^{1/3} (2K_4) P_{\text{O}_2}^{-1/4} \quad (7)$$

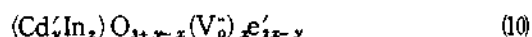
When $[\text{In}_i^+] \gg [\text{V}_\text{o}^{\bullet\bullet}]$, then

$$[e^-] = (9K_4)^{1/3} P_{\text{O}_2}^{-1/6} \quad (8)$$

$$[\text{V}_\text{o}^{\bullet\bullet}] = K_4 (9K_4)^{-1/4} P_{\text{O}_2}^{-1/4} \quad (9)$$

Under these conditions $[\text{V}_\text{o}^{\bullet\bullet}]$ increases with decreasing oxygen pressure. In the present work, we observed that the oxygen pressure dependence of electrical conductivity for pure In_2O_3 is $-0.18(\pm 0.005)$ at 800°C. This result supports that the predominant defect is triply-charged interstitial indiums. Namely, at high temperatures new donor level is produced by the transfer of In in In_{In} to interstitial sites.

On the basis of the above results, we can analyze the electrical properties of the Cd-doped In_2O_3 system as follows. When small amounts of CdO are added to In_2O_3 , the Cd atoms enter substitutionally in the cation lattice. Cd^{2+} can act as an electron acceptor and then the system can be described by



As shown in Figure 5, thermoelectric power shows that all the specimens have negative Seebeck coefficients, indicating electrons serve as the carriers, which change rather sharply with low CdO mol %. The ratio of carrier density in highly doped In_2O_3 to that in lightly doped In_2O_3 decreases as the impurity density increases and finally the carrier density reaches a saturated value. These results can be explained in the following ways: If the doped Cd ions are compensated by native donors which are produced in the In_2O_3 , donor concentration would be almost the same as the concentration of doped Cd atoms and the electrical properties would not change above a certain concentration of CdO. Moreover, it can't also be excluded that in highly doped specimens aggregation of impurity atoms can occur, thus reduce appreciably the effect of the dopant.

The electrons as carrier might be trapped in oxygen vacancies until the electrons obtain sufficient energy for excitation to the conduction band. In the 4.8 mol % Cd-doped In_2O_3 system, activation energies calculated in the high- and low-temperature region are 1.59 and 0.24 eV, respectively, at 10^{-1} atm of P_{O_2} . The activation energy from the intrinsic region contains a contribution from the energy for the formation of the $\text{In}_i^{\bullet\bullet}$ which is in turn responsible for electrical conduction, as well as a contribution from the energy for migration. In the extrinsic range the activation energy is assumed to be the sum of the energy for the excitation of the electron to the conduction band and the energy for the migration of the carrier. Since oxygen vacancies already exist in the speci-

men as native donors and the energy for migration of electron trapped in an oxygen vacancy is very small (~ 0.01 eV), the activation energy in the extrinsic region may be less than that in the intrinsic region. When the formation of interstitial indiums is begun, the extrinsic region may disappear. Then the activation energy in the intrinsic region must have a larger value than that in the extrinsic region. Consequently, the electrical conduction in the intrinsic region contains the formation of new donor level (In_i^+) represented as Eq. (5). In the extrinsic region, it is believed from the viewpoint of the activation energy (0.24 eV) that electron carriers itinerate in the conduction band. Both Zn¹⁸ and Sn-doped In₂O₃^{15,19} show increased conductivity as compared to undoped In₂O₃, but Cd-doped In₂O₃ shows decreased conductivity compared to pure In₂O₃ as shown in Figure 4. In other words, the Cd-dopant decreases the electrical conductivity. The increase in CdO mol % decreases the electrical conductivity. This result enables us to consider that the incorporated Cd inhibits the ionization of In_i^+ to In_i^+ , and results in the decrease of the concentration of conduction electron and electrical conductivity with increasing CdO mol %.

Acknowledgement. We are grateful to the Korea Science and Engineering Foundation for financial support. We also thank Professor Robert G. Sauer, Department of Physics, Yonsei University for useful discussion.

References

1. L. C. Schmacher, S. Mamichi-Afara, and M. J. Dignam, *J. Electrochem. Soc.*, **133**, 716 (1986).
2. D. Laser, *J. Appl. Phys.*, **52**, 5179 (1981).
3. K. Otsuka, T. Yasui, and A. Morikawa, *Bull. Chem. Soc. Jpn.*, **55**(6), 1768 (1982).
4. S. H. Lee, G. Heo, K. H. Kim, and J. S. Choi, *Int. J. Chem. Kinetics*, **19**(1), 1 (1987).
5. Z. Ovadyahu, B. Ovrin, and H. W. Kraner, *J. Electrochem. Soc.*, **130**(4), 917 (1983).
6. J. H. W. de Wit, *J. Sol. Sta. Chem.*, **8**, 142 (1973).
7. J. H. W. de Wit, *ibid.*, **13**, 192 (1975).
8. Y. Kanai, *Jpn. J. Appl. Phys.*, **24**(5), L361 (1985).
9. W. R. Runyan, "Semiconductor Measurements and Instrumentation", McGraw-Hill Co., New York, p.65, 1975.
10. J. F. McCan and J. O. M. Bockris, *J. Electrochem. Soc.*, **128**, 1719 (1981).
11. R. L. Weiher and B. G. Dick, *J. Appl. Phys.*, **35**(12), 3511 (1964).
12. A. K. Vijn, *J. Phys. Chem. Solids*, **29**, 2233 (1969).
13. I. Hamberg and C. G. Granqvist, *J. Appl. Phys.*, **60**(11), R123 (1986).
14. J. H. W. de Wit, G. van Unen, and M. Lahey, *J. Phys. Chem. Solids*, **38**, 819 (1977).
15. J. L. Bates, C. W. Griffin, D. D. Marchant, and J. E. Granier, *Am. Ceram. Soc. Bull.*, **65**(4), 673 (1986).
16. A. Gupta, P. Gupta, and V. K. Srivastava, *Thin Solid Films*, **123**, 325 (1985).
17. C. A. Pan and T. P. Ma, *Appl. Phys. Lett.*, **37**(163), 714 (1980).
18. R. L. Weiher, *J. Appl. Phys.*, **33**(9), 2834 (1962).
19. Y. Kanai, *Jpn. J. Appl. Phys.*, **23**(1), L12 (1984).
20. C. A. Pan and T. P. Ma, *J. Electrochem. Soc.*, **128**(9), 1953 (1981).

Reaction of Triethylsilyl Radical with Sulfides, a Laser Flash Photolysis Study

M. S. Platz¹

Ohio State University, Department of Chemistry, 140W. 18th Avenue Columbus, OH, 43210

Woobung Lee*

Department Chemistry, Kyungpook National University, Daegu 635. Received May 8, 1989

Triethylsilyl radical was generated by laser flash photolysis of a 1:1 (v/v) solution of triethylsilane and di-*tert*-butyl peroxide. The silicon centered radical was reacted with sulfides to give carbon centered radicals by displacement at sulfur. The carbon radicals were readily detected by their transient absorption spectra. The absolute rate of reaction of triethylsilyl radical with 9-fluorenylphenylsulfide, di-*n*-butylsulfide, di-*sec*-butyl sulfide, di-*tert*-butyl sulfide and di-*n*-butyl disulfide are $2.40 \pm 0.12 \times 10^8 \text{ M}^{-1}\text{s}^{-1}$, $11.21 \pm 0.89 \times 10^6 \text{ M}^{-1}\text{s}^{-1}$, $8.79 \pm 0.73 \times 10^6 \text{ M}^{-1}\text{s}^{-1}$, $3.29 \pm 0.18 \times 10^6 \text{ M}^{-1}\text{s}^{-1}$, and $3.41 \pm 0.09 \times 10^8 \text{ M}^{-1}\text{s}^{-1}$, respectively.

Introduction

Silicon and tin centered radicals rapidly abstract halogen atoms from alkyl halides to generate carbon centered radicals.² This approach has been used numerous times to gene-

rate organic radicals for study by EPR or laser flash photolysis, or for use in organic synthesis. One of the more common approaches is to photolyze a solution of di-*tert*-butyl peroxide (DTBP) and triethylsilane containing a halogen atom donor RX. Under these conditions R· can be can be